Mapping Heavy Metals in Sediment from Aswan Reservoir Using GIS Geo-statistical Analyst

Hala M. Ebaid [1] and Salwa M. Abou ElElla [2]

[1] Survey Research Institute, National Water Research Center, 308 El Harm S., Giza, Egypt;
[2] Channel Maintenance Research Institute, National Water Research Center, Cairo, Egypt;
E-Mails: hala_srif@yahoo.com, salwaabouelella@yahoo.com

Abstract: Evaluation, analyzing spatial variability of Heavy metals (HM) concentration in sediment of Aswan Reservoir was carried out. Samples were collected and tested for determining the true concentrations of: Copper (Cu), Zinc (Zn), Manganese (Mn), Lead (pb), and Iron (Fe) through 2009. Ggeostatistical analyst tools were used to explore this data, test spatial interpolation methods, analyze spatial distribution and autocorrelation of HM concentration, and finally predicted HM concentrations maps. The results reveals that Ordinary Kriging was the best method for prediction HM maps based on RMS errors and R^2. Also J-bessel was selected as the best fitted Semivariogram model for almost all HM data set. The results also demonstrated that Fe and Cu have strong spatial dependence structure 8.7%, 15%, while Zn and Mn have moderate and week spatial dependence respectively (38.48%, 99%). Also effective range of most HM parameters is close together with the range of 0.972 to 1.641 km. Top eastern parts of study area have higher concentration of Cu, and Mn pollution due to man's activities, while top western parts have higher concentration of Fe, and Zn pollution due to presence of rocks. Lead pollution map was interpolated using Inverse Distance Weighted because it was detected in little specific locations.
Hala M. Ebaid and Salwa M. Abou ElElla. Mapping Heavy Metals in Sediment from Aswan Reservoir Using GIS Geo-statistical Analyst. J Am Sci 2014;10(5):108-115]. (ISSN: 1545-1003). http://www.jofamericanscience.org. 15

Keywords: Heavy metals; GIS; Geo-statistics; Aswan reservoir; Ordinary Kriging

1. Introduction

Heavy metals enter lakes or reservoirs from a variety of sources, such as:(1) rocks and soils directly exposed to surface water; this is the largest natural sources, (2) Dead and decomposed vegetation and animal matter, contribute small amounts of metals to adjacent waters, (3) Wet and dry fallout of atmosphere particulate matter arrived from natural sources, and (4) from man's activities, including the discharge of various treated and untreated liquid wastes into the water body [1].

Trace elements, such as Cu, Zn, Mn and Fe play an essential biochemical role in the life processes in the aquatic environment. On the other hand, Pb is non-essential element and considered to be very toxic to the environment [2,3]. Pollution mapping is a time consuming process that requires the intense efforts of scientists to think spatially, geographically, technically, and statistically to produce an accurate prediction map. To understand and solve a problem, particularly in the geo-environmental sciences, broad interdisciplinary knowledge of basic sciences, environmental science, geospatial statistical analysis, GIS, and analytical aptitude are necessary requirements [4]. Also, due to cost and practicality, it is not feasible to establish monitoring stations in every location of study area to measure the pollutant concentration. Therefore, prediction of values at other locations based upon selectively measured values could be one of the alternatives [5].

There are two main groupings of interpolation techniques: deterministic and geostatistical. Deterministic interpolation techniques create surfaces from measured points, based on either the extent of similarity (e.g. Inverse Distance Weighted (IDW)) or the degree of smoothing (e.g. radial basis functions). Geostatistical interpolation techniques (e.g. kriging) utilize the statistical properties of the measured points. Using measured sample points from a study area, geostatistics can create prediction for other unmeasured locations within the same area. The geostatistical techniques quantify the spatial autocorrelation among measured points and account for the spatial configuration of the sample points around the prediction location [6]. The main advantage of using Kriging in spatial interpolation is its ability to calculate the uncertainty of prediction which is useful in decision making. A Kriging Interpolation model predicts surfaces better than other models when data are checked for outliers and errors [9]. If the data follow a normal distribution, Kriging is the best unbiased method of predicting a surface [9]. The accuracy of interpolation methods for spatially predicting soil and water properties has been analyzed in several studies [10-12].

Thus this research has been done to monitor and analyze the spatial patterns of HM elements in the Old Aswan reservoir sediments using ArcGIS Geostatistical Analyst. A set of geo-statistical techniques including those for exploratory spatial

data analysis, structural analysis, and surface prediction and assessment were conducted. The HM concentration maps were developed using these techniques to provide valuable information and risk management decision-making.

2. Study area

The study area is between High Aswan Dam and Old Aswan reservoir. Aswan High Dam was constructed on Nile River 7.00 km upstream old Aswan reservoir. The study area lies between the longitudes of 32°51'42.642"E to 32°53'57.778"E and latitudes 23°58'59.827"N to 24°1'54.911"N (Fig. 1). This area of reservoir is mostly surrounded by rocky terrain.

3. Materials and methods

3.1 Sampling and laboratory Analysis of heavy metals concentrations

Samples were taken directly from 16 sites from surficial sediment (approximately the upper 5 cm) from reservoir, in September 2009 using Ekman grab method. Each sediment sample was air-dried in the laboratory at room temperature and passed through 2 mm sieve prior to extraction. The dry weight of each sample was measured after 12 h of drying in an oven at 105°C. The sediment samples were extracted using a method modified [13]. Briefly, 1 g of each sample was placed into a 200 ml flask, then 0.2 ml sulfuric acid, 1 ml nitric acid, and 5 ml perchloric acid were added. This mixture was heated at 180°C for 3 hours on a hotplate. After the mixture cooled, 1 g ammonium chloride and 20 ml 0.5 N HCl were added. The samples were then reheated at 180°C for 1 hour and evaporated to a volume of ~10 ml. After the samples cooled, they were filtered into plastic bottles through ash-less filter paper 5B. Finally 1 ml lanthanum chloride (atomic absorption spectrometry grade, 100g-La/L solution) was added. The sample volume was standardized to 100 ml using 2% HNO_3.

3.2 Interpolation Procedures

3.2.1 Comparison of interpolation methods

First of all the interpolation method must be identfy. A cross-validation approach is used to assess the performance of Ordinary kriging (OK), and Inverse Distance Wight (IDW). The comparison criteria used are mean bias error (MBE), root mean square error (RMSE) and determination coefficient (R^2). Mathematical formula for MBE and RMSE are given as:

$$MBE = \frac{1}{N}\sum_{i=1}^{N}\left[z^*(x_i) - z(x_i)\right] \quad (1)$$

$$RMSE = \sqrt{\frac{1}{N}\sum_{i=1}^{N}\left[z^*(x_i) - z(x_i)\right]^2} \quad (2)$$

Where $z^*(x_i)$ and $z(x_i)$ are the estimated and observed values at location x_i, respectively and N is the number of observations. For an appropriate estimator, MBE should be close to zero, R^2 should be close to 1 and RMSE should be as small as possible. From this point OK was chosen for its satisfying the MBE and RMSE criteria.

3.2.2 Data exploration

The preliminary step of Geostatistical analysis is exploratory data analysis, in which the histogram, normality, trend of data, Semivariogram cloud and cross covariance cloud of the raw data were observed [14,15].Trend analysis is very important because it can help in identifying global trends in the input datasets and provides a three dimensional perspective of the point data.

3.2.3 Geostatistical techniques

Many methods are associated with geostatistics, but they are all in the kriging family. Kriging is divided into two distinct tasks: quantifying the spatial structure of the data and producing a prediction. Quantifying the structure, known as variography, is where a spatial-dependence model is fitted to data set. To make a prediction for an unknown value for a specific location, kriging will use the fitted model from variography, the spatial data configuration, and the values of the measured sample points around the prediction location. According to the theory of regionalized variable, the value of a random variable Z at a point x is given as below by [16]:

$$Z(x) = m(x) + \varepsilon'(x) + \varepsilon'' \quad (3)$$

where m(x) is the deterministic function describing the structural component of Z at point x, $\varepsilon'(x)$ is the term denoting the stochastic, locally varying but spatially dependent residual from m(x) called the regionalized variable, and ε'' is the residual having zero mean. If there is no trend in a region, m(x) equals the mean value in the region. Therefore, the expected difference between any two points x and x + h separated by a distance vector h will be zero. That is:

$$E[Z(x) - Z(x+h)] = 0 \quad (4)$$

Where Z(x) and Z(x + h) are the values of the random variable Z at point x and x + h. It also assumed that the variance of differences depends only on the distance h between points, so that:

$$E[\{z(x) - z(x+h)\}^2] = E[\{\varepsilon'(x) - \varepsilon'(x+h)\}^2] = 2\gamma(h \quad (5)$$

The term $\gamma(h)$is called semivariance. The equation (3) can be written as:

$$Z(x) = m(x) + \gamma(h) + \varepsilon'' \quad (6)$$

To show the equivalence between $\varepsilon'(x)$ and $\gamma(h)$. Thus, the semivariogram may be mathematically described as the mean square variability between two neighboring points of distance h as shown in Eq. 5 [16].:

$$\gamma(h) = \frac{1}{2N(h)} \sum_{i=1}^{N(h)} [z(x_i + h) - z(x_i)]^2 \quad (7)$$

Where γ (h) is the semivariogram expressed as a function of the magnitude of the lag distance or separation vector h between two pints, N(h) is the number of observation pairs separated by distance h and z (x_i) is the random variable at location xi.

3.2.4 Efficiency evaluation of estimator

The validation and the sufficiency of the developed model variogram can be tested via a technique called cross validation. This test allows assessing the goodness of fitting of the variogram model, the appropriateness of neighbourhood and type of kriging used. The interpolation values are compared to the real values and then the least square error models are selected for regional estimation [17]. Criteria that were used to compare the observed and estimated values including RMSE and MBA which are calculated by the equations 1 and 2 respectively. Whatever RMSE and MBA criteria closer to zero indicate a more accurate and less error of method [18].

4. Results and Discussion

In this research HM samples data of year 2009 only was examined using Geostatistical tools.A comparison between the OK and IDW was conducted as a first step by comparing the deviation of estimates from the measured HM data through using cross-validation statistics (MBE, RMSE, and R^2), table 1 describe this comparison.

The statistical results reveal that there was a better performance of OK than IDW for all items. Therefore ordinary kriging method has been used for analyzing and mapping HM parameters. A statistical summary of the HM concentration (without transformation) is presented in table 1, as a first step in data exploration. It can be noticed that the mean values of all heavy metals concentration were less than the national guideline values of lake surface sediment quality, were the limit values are 33, 95, 770,41000, and 19 For Cooper, Zinc, Manganese, Iron, and Lead respectively.

Table 2 (before transformation) clarify that the median and mean values of Cu, Zn, Mn were almost similar specially Cu and Zn, and they have relatively small Skewness values, while Iron has remarkable difference between mean and median values,and has high Skewness value. Table 3 demonstrate HM parameters values after log transformation and it is clear that the Skewness values were slightly minimized for the Cu, Zn, and Mn, while Fe Skewness value changed (from 1.456 to 0.663), and the mean and median values for Fe became almost similar after transformation. During assessment of cross validation for statistical errors it was noticed that for best fitted interpolated model and best cross validation results,only Iron needed to be transformed to the logarithmic values, which agree and confirm the above analysis. For lead parameter, it was detected in 6 sites.

Next, trend was examined; figure 2 demonstrate the global trends of data in 2009. X, Y and Z represent E, N and vertical direction respectively; black lines are samples values; green and blue lines are trends. It can be notice that Iron and Zinc concentration exhibit a strong trend in west (W)-east (E) direction, which represented as green line in the figure below, iron concentration starts out with low values, increases as it moves toward the center of the x-axis, then decreases, while the zinc concentration was represented as more pronounced U shape on x-axis (fig 3), and blue line which represent the trend in north(N) –south(S) direction is increasing as it moves towards the north (low trend for Iron and Zinc). Copper and Manganese concentration exhibit a week trend in E- W and in N –S directions. This trend consider as a nonrandom (deterministic) component of a predicted surface that can be represented by a mathematical formula (ex: second order polynomial that creates a U shape). For Lead, the figures demonstrate that in many sample locations the lead were not detected but there were trend in the two directions and the high values were detected in the east direction.

Correlation analyses have been widely applied in environmental studies. They provided an effective way to reveal the relationships between multiple variables in order to understand the factors as well as sources of chemical components between heavy metals and reflect that the accumulation concentrations of these heavy metals came from similar pollution sources [19, 20]. The concentrations of Cooper, Zinc, Manganese, Iron showed moderate positive relationship with each other and this proof that Cu, Zn, Mn, and Fe come from the same source of pollution. However, the concentration of Lead showed very weak correlations with the concentrations of the other metals.

In this study, OK was used to produce the spatial patterns of heavy metals.The Semivariogram models (circular, spherical, exponential, gaussian, rational quadratic, Hole effect, K-Bessel, and stable) were tested for each parameter of HM data set. Prediction performances were assessed by cross validation, which examines the accuracy of the generated surfaces. Table 4 lists cross validation results to examine the validity of the fitting models and parameters of semivariograms for Copper data (2009) as an example. It was clear that Copper concentration values fit Gaussian model with default

parameters (without data transformation or trend removal) because it provides most suitable model based on this criteria: less root mean square error, the mean error should be close to 0, and the root-mean square standardized error should be close to 1 [6].

Analysis has been conducted for HM data using OK with default parameters (spherical model+ No transformation + No trend Analysis), and then applying OK after applying log transformation and trend analysis (if necessary). All parameters of Semivariogram model and cross validation before and after analysis were demonstrated in table 5 for each HM parameters. The ratio of nugget variance to sill expressed in percentages can be regarded as a criterion for classifying the spatial dependence of HM parameters. If this ratio is less than 25%, then the variable has strong spatial dependence; if the ratio is between 25 and 75%, the variable has moderate spatial dependence; and greater than 75%, the variables shows only weak spatial dependence [21]. The analysis illustrate that Iron and Copper have strong spatial dependence structure, while Zinc and Manganese have moderate and week spatial dependence respectively. Also effective range of most parameters is close together with the range of 972.073 to 1641.11 m.

Interpolation maps before and after analysis were shown in figure 4, were the final HM pollution maps were presented in the right side of figure 4 (a,b.c,d) below. It was observed from all resulted HM maps below that there was influence of trend analysis on their spatial distribution. For Iron: J- Bessel model was used after applying Log-transformation and trend removal (using second order polynomial as trend type and Global interpolation as a trend removal method), also it is clear that the most polluted area concentrated in the upper lift side due to presence of rocks (fig 4a), were water depth and water speed in the left side is higher than the right side due to presence of hydropower plants, and this movement of water lead to continuous erosion in this side, hence rocks is present in left side of the study area.Cooper and Manganese interpolation maps were constructed by applying first order polynomial trend type and local polynomial interpolation as a trend removal, Gauessian and J- Bessel models were applied for Copper and Manganese respectively. No log transformation were performed for Cu and Mn, were the Skewness values did not gain significantly changes after transformation. From figure 4(b,c), it can be observed that the upper right side area exhibit a highest cooper, manganese pollution due to different man's activities as: Remnants of fishing boats like gasoline, Agricultural pesticides due to little surrounding cultivated area. Zinc Interpolation map was deduced using J- Bessel model after applying trend removal (using second order polynomial as trend type and Global interpolation as a trend removal method), without log transformation also, Zinc was concentrated in the upper lift side area due to presence of rocks. For lead:due to shortage of samples, deterministic method for interpolation was more suitable for lead concentration, so IDW was selected for interpolated map generation. It was noticed also that J-bessel considered as best fitted and suitable Semivariogram model for data set with small samples numbers.

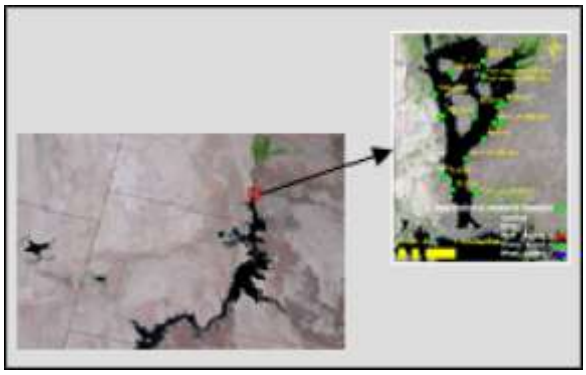

Figure 1. Location of the study area.

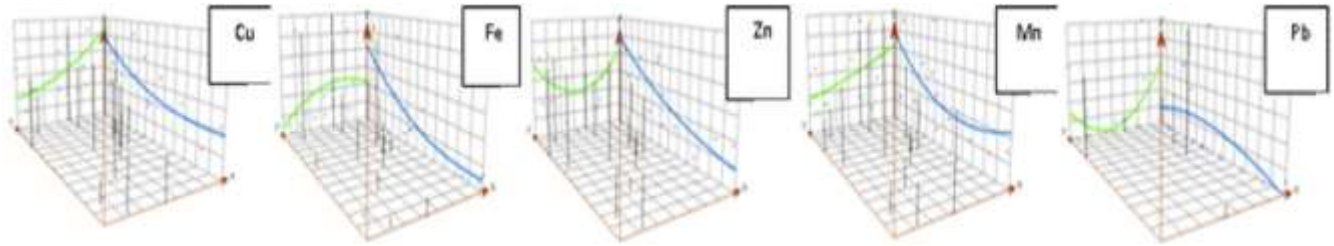

Figure 2. Global trends of Copper, Iron, Zinc, Manganese, Lead samples data in 2009.

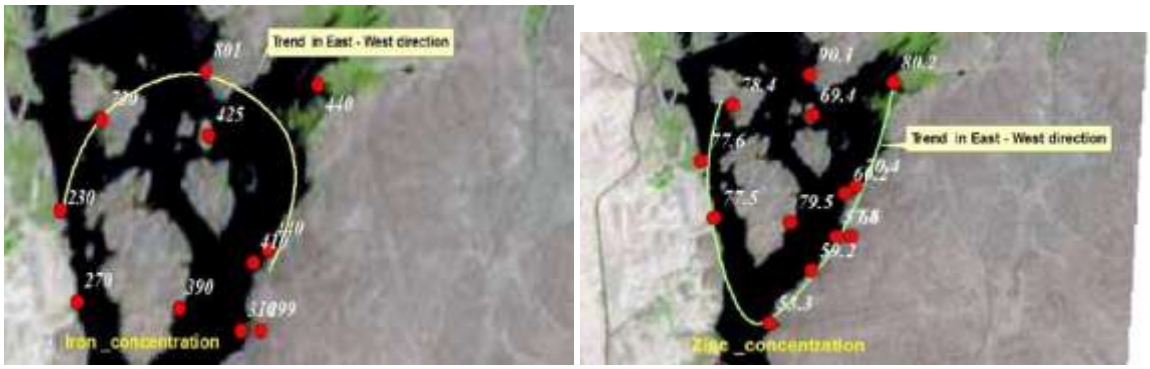

Figure 3. Iron and Zinc in E-W direction in 2009.

(a) Iron

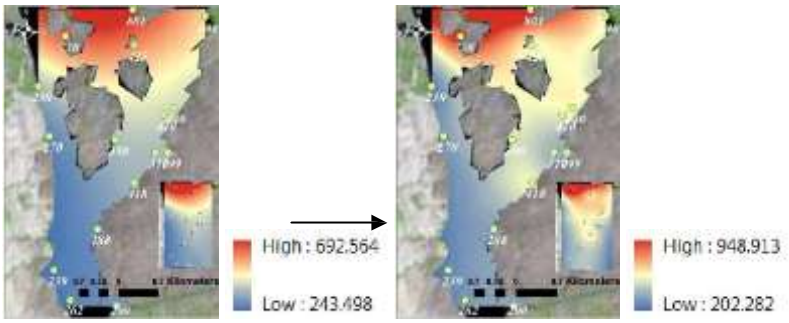

(b) Copper

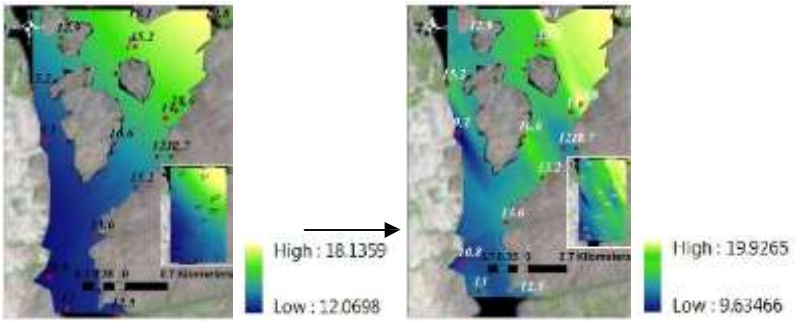

(c) Manganese

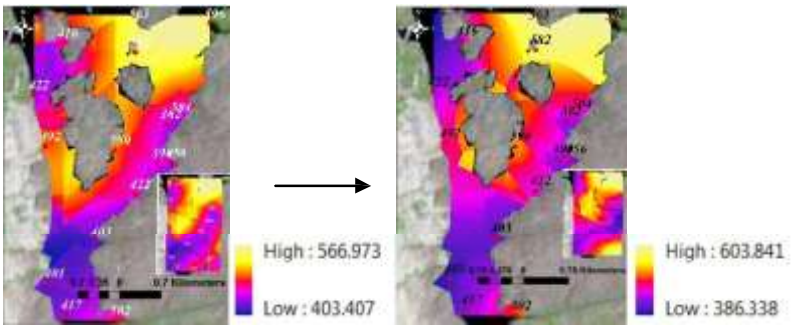

(d) Zinc

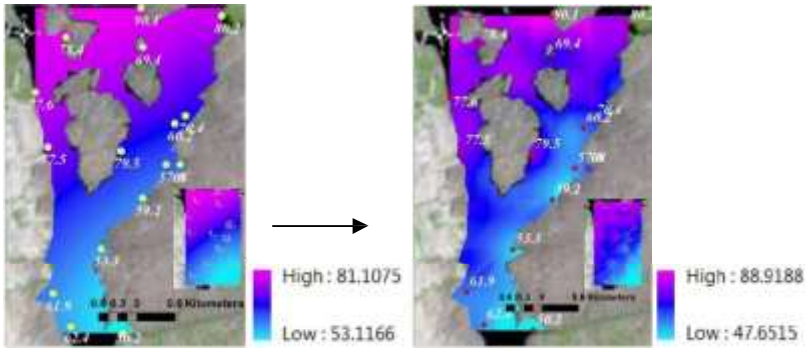

(e) Lead

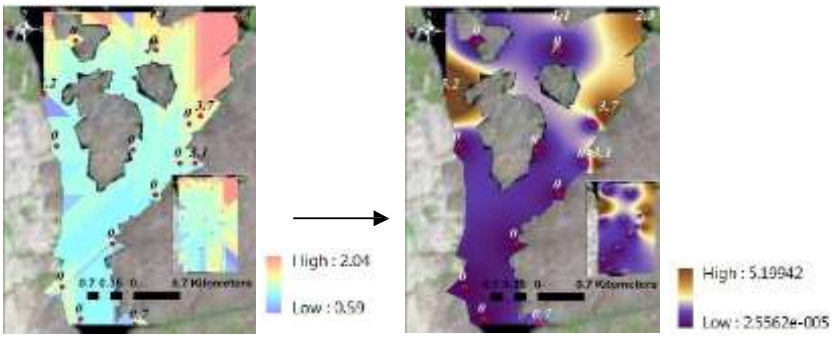

Figure 4. Interpolation maps for (a) Iron, (b) Copper, (c) Manganese, (d) Zinc, and (e) Lead data before and after analysis using O K and only for lead using IDW.

Table 1. MBE, RMSE, and R^2 for HM parameters, using OK and IDW methods

Sedm. Concentration for Heavy metals (2009)	IDW			OK		
	Mean Bias Error	RMSE	R^2	Mean Bias Error	RMSE	R^2
Copper	-0.04662	2.748	0.088	-0.02276	2.628	0.176
Zinc	-0.7053	9.819	0.244	-0.1358	7.872	0.482
Manganese	-5.422	77.6	0	-4.92	73.49	0.069
Iron	2.791	170.8	0.071	1.786	163.3	0.172
Lead	0.09158	2.665	0.251	0.04928	2.517	0.48

Table 2. Descriptive Statistics of (non-transformation) heavy metals concentration parameters (2009)

Non Transformation HM Parameters concent. (2009)	Minimum	Maximum	Mean	Median	Standard deviations	Skewness	Kurtosis	1-st quantile	3-rd Quantile
Copper	9.1	19.8	14.456	14.15	2.9721	0.26758	2.4204	12.6	15.9
Zinc	50.2	90.1	68.494	68.7	11.29	0.12827	2.0544	59.7	78
Manganese	36.2	596	469.88	439	78.305	0.44793	1.7828	409.5	533.5
Iron	230	801	390.13	350	164.56	1.4556	4.2506	279	432.5
Lead	0	8.1	1.3188	0	2.3875	1.8292	5.2634	0	1.7

Table 3. Descriptive Statistics of (Log-transformation) heavy metals concentration parameters (2009)

Log Heavy Metal Parameters concentrations (2009)	Minimum	Maximum	Mean	Median	Standard deviations	Skewness	Kurtosis	1-st quantile	3-rd Quantile
Copper	2.2083	2.9857	2.651	2.649	0.20845	0.19104	2.6918	2.5337	2.7653
Zinc	3.916	4.5009	4.214	4.2297	0.16653	-0.11605	2.0198	4.0893	4.3567
Manganese	5.8916	6.3902	6.14	6.0837	0.16334	0.30179	1.7371	6.0148	6.2779
Iron	5.4381	6.6859	5.933	5.8514	0.4007	0.66262	2.2655	5.6307	6.0868
Lead	0	8.1	1.319	0	2.3875	1.8292	5.2634	0	1.7

Table 4. Prediction errors for different models for Copper parameter (2009)

Cross Validation for copper	spherical	Exponential	Gaussian	Rational Quadratic	K-Bassel	Stable	Circular	Hole Effect
Mean	-0.05735	-0.1039	-0.02276	-0.1216	-0.03678	-0.04602	-0.04109	-0.06112
Root-Mean-Square-Error	2.663	2.788	2.628	2.914	2.65	2.674	2.629	2.718
Root-Mean-Square Standardized	0.9598	1.004	0.9486	1.041	1.017	0.9572	0.9643	0.938

Table 5. Parameters of heavy metal concentration variograms

Cross Validation	Copper		Zinc		Manganese		Iron		Lead	
	Before analysis	After analysis	Before analysis	After analysis	Before analysis	After analysis	Before analysis	After analysis	Before analysis	After analysis
Model	Spherical	Gaussian	Spherical	J-Bessel	Spherical	J-Bessel	Spherical	J-Bessel	Spherical	LDW
Mean	-0.0711	-0.0134	-0.2385	-0.4717	-0.571	-0.056	-0.147	-0.658	-0.0871	0.002
Root_Mean-Square	2.636	2.227	8.127	7.079	76.8	69.74	142.8	120.8	1.775	2.087
Root_Mean-Square Standardized	1.007	0.9923	0.9292	1.286	9613	1.513	1.237	1.709	1.022	
Nugget		0.7257		12.597		1509.8		0.002		
Partial still		4.0322		20.132		8.6862		0.026		
effective Range		1617.6		972.073		1200.5		1641		
Spatial Ratio		15%		38.48%		99%		8.7%		

5. Conclusions

From this study it can be concluded that by using Geostatistical –variogram analysis and spatial interpolation (kriging), there is possible to determine and mapped heavy metals concentration in sediment of Aswan Reservoir. The results showed that Iron and Cooper have strong spatial dependence structure 8.7%, 15%, while zinc and Manganese have moderate and week spatial dependence respectively (38.48%, 99%). Also effective range of most HM parameters is close together with the range of 0.972 to 1.641 km. Also the results reveals that J-bessel was selected as the best fitted semivariogram model for almost all HM parameters. Top eastern parts of study area have higher concentration of Cu, and Mn pollution due to different man's activities, while top western parts have higher concentration of Fe, and Zn pollution due to presence of rocks. Lead pollution map was interpolated using Inverse Distance Weighted because it was detected in little specific locations.

References

1. Nurnberg, H. W. Yoltametric trace analysis in ecological chemistry of toxic metals. Pure and Appl., Chern. 1982, 54(4), 853-878.
2. Abou Elella, S. M. Seasonal Variations of Some Heavy Metals in the Ecosystem of Nasser Lake Khors- Egypt. J. Egypt. Acad. Soc. Environ. Develop 2008, 9 (4), 1-17.
3. Abou Elella, S.M.; Hosny M.M.; Bakry, M. F. Utilizing Fish and Aquatic Weed Infestations as Bioindicators for Water Pollution in Lake Nubia, Sudan Egypt. J. Aquat. Boil. & Fish 2005, 9, 63-84.
4. Swatantra, R.; Kethireddy; Paul B.; Tchounwou; Hafiz, A. A Int. J. Environ. Res. Public Health 2014, 11, 983-1000;
5. Gorai; Kumar. Spatial Distribution Analysis of Groundwater Quality Index Using GIS: A Case Study of Ranchi Municipal Corporation (RMC) Area, Geoinfor Geostat: An Overview 2013.
6. ESRI (Environmental System Research Institute). Using ArcGIS geostatistical analyst USA 2003.
7. Chang, K.T. Introduction to Geographic Information Systems, 4th ed. McGraw-Hill Publishers, New York, NY, USA 2008, 326–356.
8. Moral, F.J.; Rebollo, F.J.; Valiente, P.; López, F.; De la Peńa, A.M. Modelling ambient ozone in an urban area using an objective model and geostatistical algorithms. Atmosph. Environ. 2012, 63, 86–93.
9. Geostatistical Analyst Tutorial; Environmental Systems Research Institute, Redlands, CA, USA, 2012, 1–57.
10. Nas, B.; Berktay, A. Groundwater contamination by nitrates in the City of Konya, (Turkey), A GIS perspective. J. of Environmental Management 2006, 79, 30-37.

11. LaMotte, A. E.; Greene, E. A. Spatial analysis of land use and shallow groundwater vulnerability in the watershed adjacent to Assateague Island National Seashore, Maryland and Virginia, USA. Environ Geol. 2007, 52, 1413-1421.
12. Barca, E.; Passarella, G. Spatial evaluation of the risk of groundwater quality degradation. A comparison between disjunctive kriging and geostatistical simulation,Environ Monit Assess 2008, 137, 261- 273.
13. Charlesworth, S.M.; Lees, J.A. The distribution of heavy metals in deposited urban dusts and sediments, Coventry, England. Environ Geochem Health. 1999, 21, 97-115.
14. Sarangi, A.; Madramootoo, C. A.; Enright P.; Chandrasekharan H. Prediction of Spatial Variability of Phosphorous Over The St-Esprit watershed, Water, Air, and Soil Polluiton. 2005,48, 3- 943.
15. Johnston, K.; Hoef J.M.V.; Krivoruchko, K.; Lucas N. Using ArcGIS Geostatistical Analyst. ESRI. 380 New York Street. Redlands, CA 92373-8100, USA. 2001.
16. Buyong, T. Spatial data analysis for geographic information science. Johor, Penerbit Universiti Teknologi Malaysia. 2007.
17. Leuangthong, O.; McLennan, J. A.; Deutsch, C. V, Minimum acceptance criteria for geostatistical realizations, Natural Resources Research, 2004, 13, 131–141.
18. Webster, R.; Oliver, M. 2001. Geostatistics for environmental science. Wiley & Sons, chichester 2001, 271.
19. Facchinelli, A.; Sacchi E.; Mallen, L. Multivariate statistical and GIS-based approach to identify heavy metal sources in soils. Environmental Pollution 2001, 114: 313–324.
20. Manta, DS.; Angelone, M.; Bellanca, A.; Neri, R.; Sprovieri, M. Heavy metals in urban soils, a case study from the city of Palermo (Sicily), Italy. The Science of the Total Environment. 2002, 300, 229–243.
21. Jiachun, Sh.; Haizhen Wang; Jianming, Xu.; Jianjun, Wu.; Xingmei, Liu.; Haiping, Zh.; Chunlan, Yu. Spatial Distribution of Heavy Metals in Soils, a Case Study of Changxing, China, Environ Geol. 2007, 52, 1-10.

4/11/2014